Journal of Physics: Conference Series

Interaction of two-frequency electromagnetic waves with anisotropic media over hydrocarbon accumulation

To cite this article: Viktar F Yanushkevich *et al* 2022 *J. Phys.: Conf. Ser.* **2373** 052016

Interaction of two-frequency electromagnetic waves with anisotropic media over hydrocarbon accumulation

Viktar F Yanushkevich, Dzmitry A Dauhiala, Aliaksandr L Adamovich, Siarhei N Abramenka and Siarhei V Kalintsau

Polotsk State University, 29, Blokhin Street, Novopolotsk, Vitebsk Region, 211440, Belarus

E-mail: v.yanushkevich@psu.by

Abstract. The article analyzes the interaction of two-frequency electromagnetic waves with anisotropic media over hydrocarbon accumulation. The behavior of the real component $\dot{\varepsilon}_3$ of the dielectric permittivity tensor is investigated. The choice of signal characteristics is based on the use of different electromagnetic wave emission sources with amplitude and frequency ratio coefficients in the modes of powerful low-frequency and high-frequency signals. The dielectric permittivity tensor component $\dot{\varepsilon}_3$ as a function of dielectric permittivity and frequency of sounding signals was analyzed. Sounding modes of anisotropic media over hydrocarbons are recommended to identify the medium over the deposits and increase the accuracy of determining the boundaries of hydrocarbon accumulation. The obtained results of the research can be used in prospecting geophysics.

1. Introduction

The relevance of this article is caused by an increase in the accuracy of determining the boundaries of hydrocarbon deposits (HC accumulations). Requirements for prospecting geophysics in modern economic conditions imply the improvement of existing and development of new methods of searching for oil and gas (hydrocarbons) based on the use of highly efficient technologies of detection of minerals [1]. Electromagnetic prospecting methods (EMP) for contouring the HC accumulations are very promising and contribute to the further development of works in this direction [2]. The proven methods of field studies [3, 4] show their high reliability in comparison with seismic, gravity, and magnetic survey methods.

Varieties of vertical sounding modes allow determining the characteristics of host rocks located above hydrocarbon deposits [5, 6]. They are differentiated by their electromagnetic properties and subsequent detection of HC accumulations. The propagation of electromagnetic waves (EMW) and their interaction with the object of research in the method of electromagnetic sounding makes it possible to obtain significantly more information about the profile of the water area [7]. Active research work on the solution of these problems is used to create equipment based on measuring resistance at the studied points of the geoprofile [8]. The set of currently available exploration results can be very useful for the development of new EMP [9].

The experience in geological exploration in prospecting geophysics shows that obtaining subsalt images in oil and gas exploration is still a difficult task. In the north of Germany, the integrated use of magnetotelluric methods was widely used in the imaging of the salt dome to improve the integration of seismic and gravimetric data [10]. The article [11] analyzes the interaction of two-frequency signals with an anisotropic medium over the HC accumulations with variation of the coefficients of the ratio of frequencies and amplitudes. In practice, a universal method for deposits monitoring and geothermal exploration can be used to solve electrical exploration problems using EMP methods [12].

The purpose of this work is to substantiate the characteristics of EMW when using two-frequency signals to qualitatively increase the level of reliability of search and identification of HC accumulations.

2. The use of two-frequency signals for electrical exploration of HC accumulations

In this work, a two-frequency EMW of the following form is used to search for hydrocarbon deposits:

$$\vec{S}(t) = \vec{S}_1(t) + \vec{S}_2(t) = A_1 \cos \omega_1 t + A_2 \cos \omega_2 t, \tag{1}$$

where $A_1, A_2, \omega_1 = 2 \cdot \pi \cdot f_1,\ \omega_2 = 2 \cdot \pi \cdot f_2$ – signal amplitudes and frequencies.

Various sources of EMW radiation with coefficients of the ratio of amplitudes and frequencies are used for electrical exploration tasks

$$k_E = \frac{A_2}{A_1},\ k_\omega = \frac{\omega_1}{\omega_2} \tag{2}$$

The propagation of two-frequency EMWs in the medium above the HC deposits in the modes of powerful low-frequency (LF) with coefficients $k_E \ll 1, k_\omega \ll 1$ and high-frequency (HF) with coefficients $k_E \gg 1, k_\omega \ll 1$ signals is considered in [3,13,14]. However, these sources do not consider the analysis of the third component of the dielectric permittivity tensor of the medium. This article is devoted to the analysis of this characteristic. The components of the dielectric permittivity tensor of the medium in the LF mode have the form [3]:

$$\begin{cases} \dot{\varepsilon}_1 = \varepsilon_r \frac{\widetilde{\omega}_1}{\omega_2} + \sum_{i=1}^{2} \begin{Bmatrix} \frac{\omega_{\Pi i}^2 \widetilde{\omega}_1}{\omega_2} \frac{\omega_{\Gamma i}^2 - \widetilde{\omega}_1^2 - {\nu_i}^2}{({\nu_i}^2 + \omega_{\Gamma i}^2 - \widetilde{\omega}_1^2)^2 + 4\widetilde{\omega}_1^2 {\nu_i}^2} - \\ -j\left[\frac{-\varepsilon_r k_E (1-k_\omega) \sin \alpha t}{1 + k_E \cos \alpha t} + \frac{\sigma_r}{\omega_2 \varepsilon_0} + \frac{\omega_{\Pi i}^2 \nu_i}{\omega_2} \frac{\widetilde{\omega}_1^2 + {\nu_i}^2 + \omega_{\Gamma i}^2}{({\nu_i}^2 + \omega_{\Gamma i}^2 - \widetilde{\omega}_1^2)^2 + 4\widetilde{\omega}_1^2 {\nu_i}^2}\right] \end{Bmatrix}, \\ \dot{\varepsilon}_2 = \sum_{i=1}^{2} \left\{ \frac{\omega_{\Pi i}^2 \omega_{\Gamma i}}{\omega_2} \frac{\omega_{\Gamma i}^2 - \widetilde{\omega}_1^2 + {\nu_i}^2}{({\nu_i}^2 + \omega_{\Gamma i}^2 - \widetilde{\omega}_1^2)^2 + 4\widetilde{\omega}_1^2 {\nu_i}^2} - \frac{2j\widetilde{\omega}_1 \nu_i \omega_{\Pi i}^2 \omega_{\Gamma i}}{[({\nu_i}^2 + \omega_{\Gamma i}^2 - \widetilde{\omega}_1^2)^2 + 4\widetilde{\omega}_1^2 {\nu_i}^2]\omega_2} \right\}, \\ \dot{\varepsilon}_3 = \varepsilon_r \frac{\widetilde{\omega}_1}{\omega_2} + \sum_{i=1}^{2} \left\{ \frac{\omega_{\Pi i}^2 \widetilde{\omega}_1}{\omega_2} \frac{1}{{\nu_i}^2 + \widetilde{\omega}_1^2} - j\left[\frac{-\varepsilon_r k_E (1-k_\omega) \sin \alpha t}{1 + k_E \cos \alpha t} + \frac{\sigma_r}{\omega_2 \varepsilon_0} + \frac{\omega_{\Pi i}^2 \nu_i}{\omega_2} \frac{1}{\widetilde{\omega}_1^2 + {\nu_i}^2}\right] \right\}. \end{cases} \tag{3}$$

Expressions (equation 3) include $\dot{\varepsilon}_1$, $\dot{\varepsilon}_2$, $\dot{\varepsilon}_3$ - tensor components; $\omega_{\Pi i}$ - plasma frequency; $\omega_{\Gamma i}$ - gyrotropic frequency; ν_i - particle collision frequency; ε_r - relative permittivity of the medium; σ_r - conductivity of the medium; ε_0 - dielectric constant; $\alpha = \omega_2 - \omega_1 = \omega_2(1 - k_\omega)$ - frequency difference of two EMWs.

The frequency component that characterizes this sounding mode

$$\widetilde{\omega}_1 = \omega_2[k_\omega + k_E^2 + k_E(1 - k_\omega) \cos \alpha t] \tag{4}$$

The method for detecting hydrocarbons is based on the analysis of the tensor component for the modes of LF and HF signals. The frequency component that sets the HF sounding mode

$$\widetilde{\omega}_2 = \omega_2 \left[k_\omega + 1 + \frac{1-k_\omega}{k_E} \cos \alpha t\right] \tag{5}$$

is a part of the corresponding tensor of dielectric permittivity of the medium above the HC deposits, the components of which in the HF mode have the form [3]:

$$\begin{cases} \dot{\varepsilon}_1 = \varepsilon_r \dfrac{\tilde{\omega}_2}{\omega_2} + \sum_{i=1}^{2} \left(\begin{aligned} & \frac{\omega_{\Pi i}^2 \tilde{\omega}_2}{\omega_2} \frac{\omega_{\Gamma i}^2 - \tilde{\omega}_2^2 - {\nu_i}^2}{({\nu_i}^2 + \omega_{\Gamma i}^2 - \tilde{\omega}_2^2)^2 + 4\tilde{\omega}_2^2 {\nu_i}^2} - j \left[\frac{\sigma_r}{\omega_2 \varepsilon_0} + \right. \\ & \left. + \frac{\omega_{\Pi i}^2 \nu_i}{\omega_2} \frac{\tilde{\omega}_2^2 + {\nu_i}^2 + \omega_{\Gamma i}^2}{({\nu_i}^2 + \omega_{\Gamma i}^2 - \tilde{\omega}_2^2)^2 + 4\tilde{\omega}_2^2 {\nu_i}^2} \right] \end{aligned} \right), \\ \dot{\varepsilon}_2 = \sum_{i=1}^{2} \left\{ \begin{aligned} & \frac{\omega_{\Pi i}^2 \omega_{\Gamma i}}{\omega_2} \frac{\omega_{\Gamma i}^2 - \tilde{\omega}_2^2 + {\nu_i}^2}{({\nu_i}^2 + \omega_{\Gamma i}^2 - \tilde{\omega}_2^2)^2 + 4\tilde{\omega}_2^2 {\nu_i}^2} - \\ & - \frac{2j\tilde{\omega}_2 \nu_i \omega_{\Pi i}^2 \omega_{\Gamma i}}{[(\nu_i^2 + \omega_{\Gamma i}^2 - \tilde{\omega}_2^2)^2 + 4\tilde{\omega}_2^2 \nu_i^2]\omega_2} \end{aligned} \right\}, \\ \dot{\varepsilon}_3 = \varepsilon_r \dfrac{\tilde{\omega}_2}{\omega_2} - \sum_{i=1}^{2} \left\{ \dfrac{\omega_{\Pi i}^2 \tilde{\omega}_2}{\omega_2} \dfrac{1}{{\nu_i}^2 + \tilde{\omega}_2^2} - j \left[\dfrac{\sigma_r}{\omega_2 \varepsilon_0} + \dfrac{\omega_{\Pi i}^2 \nu_i}{\omega_2} \dfrac{1}{\tilde{\omega}_2^2 + {\nu_i}^2} \right] \right\}. \end{cases} \tag{6}$$

Plasma frequency

$$\omega_{\Pi i} = q_i \left(\frac{N_i}{m_i \varepsilon_0} \right)^{\frac{1}{2}} \tag{7}$$

In expressions (equation 7) q_i, N_i, m_i - charge, concentration and mass of particles.

3. Research results

We have analyzed expressions (equation 3) for the tensor component $\dot{\varepsilon}_3$ in the LF mode of exposure in the frequency range $f_2 = (10^5 – 10^{10})$ Hz at the particle concentration $N_e = 10^{16}$m^{-3}, $N_i = 10^{18}$m^{-3} and the values of the dielectric constant of the medium ε_r = 10 – 30, electrical conductivity σ_r = 10^{-3} Sm/m, particle collision frequency $\nu = 2 \cdot \pi \cdot 10^9$ rad/s (for electron-ion conductivity).

Studies of the real component of the tensor component $\dot{\varepsilon}_3$ (figure 1, figure 2) at variation of dielectric permittivity of the medium and coefficients of the amplitude-frequency ratio were carried out. On the graphs, the values of the second index correspond to the values: without the index – ε_r = 10, 1 – ε_r = 20, 2 – ε_r = 30. It was found that at low sounding frequencies (10^5 Hz - 10^7 Hz) for $k_\omega = 10^{-1}, k_E = 10^{-1}$, $N_e = 10^{16}$ m^{-3}, $N_i = 10^{18}$ m^{-3}, the real component of the tensor component $\dot{\varepsilon}_3$ takes practically constant positive values. The same pattern is observed on the frequency segment The same pattern is observed on the frequency segment $f_2 = (2 \cdot 10^9$ Hz – $1 \cdot 10^{10}$ Hz). The range of the HF component of the two-frequency signal $f_2 = (2 \cdot 10^7$ Hz – $2 \cdot 10^9$ Hz), characterized by a sharp decrease in the considered component of the dielectric permittivity tensor of the medium over the HC deposits is of interest. When the dielectric permittivity changes from 10 to 30, the real component of the tensor component retains the characteristic change with increasing numerical values. The dependences of the component Re $\dot{\varepsilon}_3$ on the high-frequency component of the signal for $k_\omega = 10^{-1}, k_E = 10^{-1}$, $N_e = 10^{16}$ m^{-3}, N_i=10^{17} m^{-3} have differences from the mode considered above. First, the range of values of the real component of the tensor in the entire range of frequencies under study is much smaller than in the previous case. Second, the frequency range of the values of the real component of the tensor $\dot{\varepsilon}_3$ is much smaller. Thus, for low sounding frequencies (10^5 Hz – $4 \cdot 10^7$ Hz) for $k_\omega = 10^{-1}$, $k_e = 10^{-1}$, $N_e = 10^{16}$ m^{-3}, N_i=10^{17} m^{-3} the real component of the tensor component takes practically constant values. The same pattern is characteristic of the process of propagation of two-frequency electromagnetic waves over anisotropic media over HC deposits on the frequency interval $f_2 = (10^9$ Hz –10^{10} Hz). Of interest is the mode characterized by a sharp increase in the considered component of the dielectric permittivity tensor of the medium over the HC accumulations in the range of the HF component of the two-frequency signal f_2 = ($4 \cdot 10^7$ Hz – $1 \cdot 10^9$ Hz).

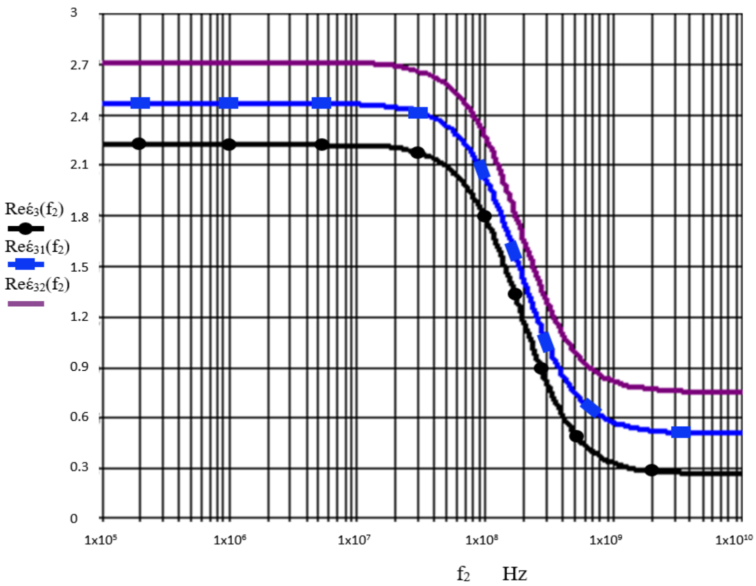

Figure 1. Dependencies of the Re $\dot{\varepsilon}_3$ component on the high-frequency component of the signal for $k_\omega = 10^{-1}, k_E = 10^{-1}$, $N_e = 10^{16}$ m^{-3}, $N_i = 10^{18}$ m^{-3}.

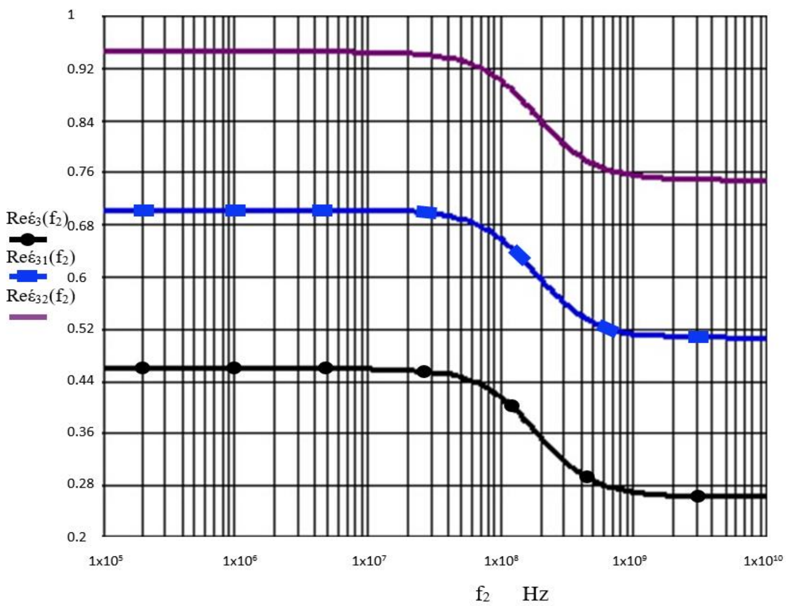

Figure 2. Dependencies of the Re $\dot{\varepsilon}_3$ component on the high-frequency component of the signal for $k_\omega = 10^{-1}, k_E = 10^{-1}$, $N_e = 10^{16}$ m^{-3}, $N_i = 10^{17}$ m^{-3}.

When the dielectric permittivity changes from 10 to 30, the real component of the tensor component $\dot{\varepsilon}_3$ retains the characteristic change with decreasing numerical values.

The analysis of expressions (equation 6) for the tensor component $\dot{\varepsilon}_3$ in the HF exposure mode in the frequency range $f_2 = (10^5 - 10^{10})$ Hz at particle concentrations $N_e = 10^{16}$ m^{-3}, Ni = 10^{18} m^{-3} (figure 3), $N_e = 10^{16}$ m^{-3}, $N_i = 10^{17}$ m^{-3} (figure 4) and values of dielectric permittivity of the medium $\varepsilon_r = 10 - 30$, electric conductivity σ_r = 10^{-3} Sm/m, and particle collision frequency $\nu = 2 \cdot \pi \cdot 10^9$ rad/s (two-particle electron-ion medium is considered).

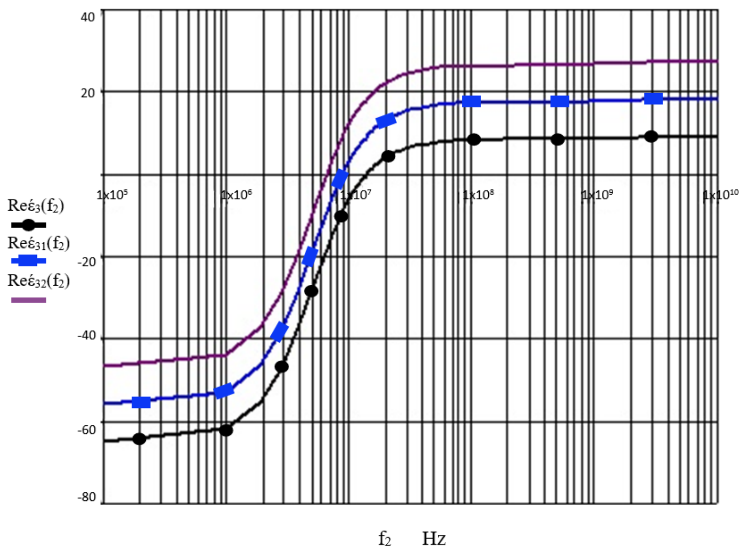

Figure 3. Dependencies of the Re $\dot{\varepsilon}_3$ component on the high-frequency component of the signal for $k_\omega = 10^{-6}, k_E = 10$, N_e = 10^{16} m^{-3}, N_i = 10^{18} m^{-3}.

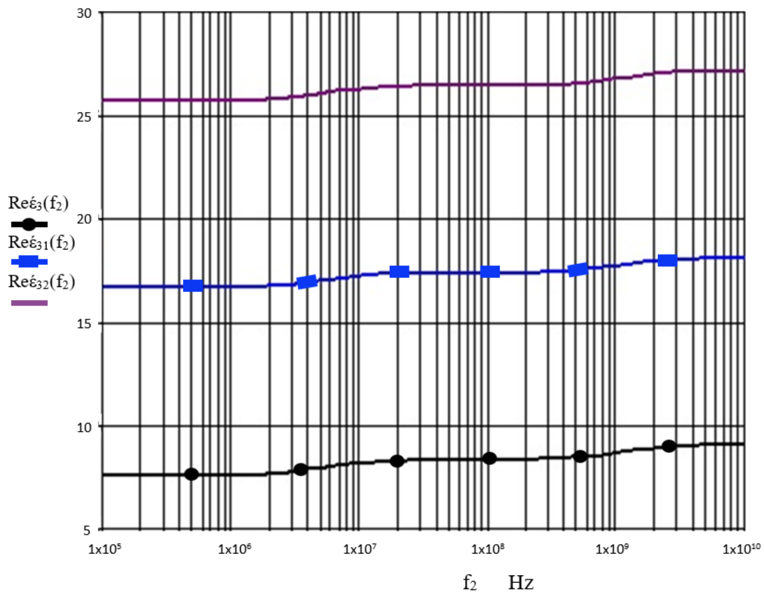

Figure 4. Dependencies of the Re $\dot{\varepsilon}_3$ component on the high-frequency component of the signal for $k_\omega = 10^{-6}, k_E = 10$, Ne = 10^{16} m^{-3}, Ni=10^{16}m^{-3}.

The real component of the tensor component in the HF exposure mode at particle concentrations of N_e = 10^{16} m^{-3}, N_i = 10^{18} m^{-3} has points of transition through zero at the interval f_2 = (5 – 15) MHz at concentrations of particles N_e = 10^{16} m^{-3}, N_i = 10^{17} m^{-3} an insignificant increase in this component is observed at intervals f_2 = (2 – 20) MHz and f_2 = ($2 \cdot 10^8$ – $2 \cdot 10^9$) Hz. The conducted research extends the database for diagnostics of anisotropic media above the HC deposits, taking into account the contribution of mineralogical and granulometric properties, the skeleton features of reservoir rocks.

4. Conclusion

The analysis of two-frequency EMW interaction with anisotropic media over HC deposits in LF and HF signal modes showed:

- In the mode of low-frequency exposure the range of the HF component of the two-frequency signal $f_2 = (2\cdot10^7$ Hz – $2\cdot10^9$ Hz) at particle concentrations of $N_e = 10^{16}$ m^{-3}, $N_i = 10^{18}$ m^{-3}, characterized by a sharp change in the real component of the dielectric permittivity tensor of the medium over the HC deposits, is of interest;
- In the mode of high-frequency exposure a sharp increase in the material component of the tensor component $\dot{\varepsilon}_3$with transition through zero at the interval f_2 = (5 – 15) MHz at particle concentrations of $N_e = 10^{16}$ m^{-3}, $N_i = 10^{18}$ m^{-3} is observed.

References

[1] Khmelevskoy V K, Gorbachev Y I, Kalinin A V, Popov M G, Seliverstov N I and Shevnin V A 2004 *Geophysical research methods: handbook for geological specialties of universities* (Petropavlovsk-Kamchatsky: Publishing House of KSPU)
[2] Gololobov D V 2008 Radio complexing of electromagnetic exploration methods in the search for hydrocarbon deposits *BSUIR* **8(38)** 30-6
[3] Yanushkevich V F 2017 *Electromagnetic methods of search and identification of hydrocarbon deposits* (Navapolatsk)
[4] Khmelevskoy V K and Bondarenko V M 1989 *Electrical exploration: reference. geophysics* **2** ed. and additional Khmelevskoy V K and Bondarenko V M (Moscow:Nedra)
[5] Helwig S L, Wood W and Gloux B 2019 Vertical-vertical controlled source electromagnetic instrumentation and acquisition *Geophys. Prospect.* **67(6)** 1582-94
[6] Holten T, Luo X, Naevdal G and Helwig S L 2016 Time lapse CSEM reservoir monitoring of the Norne field with vertical dipoles *SEG Technical Program Expanded Abstracts* **35** 971-5
[7] Palshin N A 2009 Problems of electromagnetic sounding in water areas *Geophysical Journal* **31** 4-8
[8] Petrov A A, Malovichko M S, Kocherov A B and Lisitsyn E D 2010 The experience of using electromagnetic sounding in the search for hydrocarbons in the transit zone of the Caspian Sea *Geophysics* **2** 60-4
[9] Vladov M L 2004 *Introduction to georadiolocation* ed Vladov M L and Starovoitov A V (Moscow: Publishing House of Moscow State University) 153
[10] Henke C H, Krieger M, Strack K and Zerilli A 2020 Subsalt imaging in Northern Germany using multi-physics (magnetotellurics, gravity, and seismic) *Interpretatio* **8(4)** 15-24
[11] Yanushkevich V F, Dauhiala D A, Adamovich A L *et al.* 2021 Effect of a powerful low-frequency signal on an anisotropic medium over hydrocarbon *Journal of Physics: Conference Series* **1889** 22-59
[12] Geldmacher I A and Strack K 2017 Fit-for-purpose electromagnetic System for Reservoir Monitoring and Geothermal Exploration *GRC Transactions* **41** 1649-58
[13] Yanushkevich V F, Kalintsau S V and Bogush V A 2021 Application of two-frequency electromagnetic waves to determine the properties of the medium over hydrocarbons *Bulletin of Polotsk State University Ser. C Fundamental Sciences* **4** 65-71
[14] Yanushkevich V F, Abramenka S N, Kalintsau S V and Bogush V A 2021 High-frequency sensing modes using two-frequency signals to search for hydrocarbons *Bulletin of Polotsk State University Ser. C Fundamental Sciences* **4** 77-82